Thermoluminescence Theory and Analysis: Advances and Impact on Applications

Y Horowitz, Ben-Gurion University of the Negev, Beersheva, Israel
R Chen, Tel Aviv University, Tel Aviv, Israel
L Oster, Sami Shamoon College of Engineering, Beersheva, Israel
I Eliyahu, Ben-Gurion University of the Negev and SOREQ Nuclear Research Center, Yavne, Israel

Historical Background

Thermoluminescence (TL) also called as thermally stimulated luminescence refers to a process in which a solid, usually in crystalline form, emits light while being heated following excitation. Although the excitation is most often by ionizing or non-ionizing radiation, it can also occur via pressure (piezo-TL), friction (tribo-TL), or light (photo-TL). The latter three modes are usually considered "spurious TL." The emitted light intensity $I(T)$, recorded as a function of temperature, is commonly referred to as a "glow curve" and is composed of one or more glow peaks. Each glow peak can, ideally, be associated with a particular electron or hole trapping center (TC). TL seems to have been discovered by Robert Boyle who, in 1663, described to the Royal Society one of the first accounts of TL in which he described heating a diamond with the words "I also brought it to some kind of glimmering light, by taking it into bed with me, and holding it a good while upon a warm part of my naked body." The intensive study of TL started in the first half of the 20th century. For example, in 1927, Wick reported on the TL of X-ray irradiated fluorite and other materials. The first quantitative theoretical account, based on the model of energy bands in crystals, was developed in 1945 in a seminal work by Randall and Wilkins. Since then, many books have been written in the past half century on the characteristics and theory of TL in substantial detail, for example, by Horowitz in 1984; McKeever, Moscovitch, and Townsend in 1995; and Chen and Pagonis in 2011. For those wishing an even greater mental challenge and extended physical insights, the readers are referred to Bräunlich.

Conduction Band/Valence Band Model

Many TL mechanisms are interpreted using the energy-band theory of solids. Following irradiation, charge carriers (both electrons and holes) are trapped in allowed states in the forbidden gap, which are associated with impurity or defect-created imperfections. The energy absorbed during excitation liberates electrons and holes that are free to migrate in the conduction and valence bands, respectively, and then to be trapped in the electron and hole allowed states. The energy levels of the traps may be sufficiently close to the bands so that the trapped charge carriers will be thermally released into their respective bands during heating.

The trapping states farthest from their respective bands are most likely to result in recombination of a mobile carrier and a trapped charge of the opposite sign, and these are usually referred to as "recombination centers" or simply "centers." Thus, during the readout stage, mobile charge carriers, either electrons or holes, can recombine with charges of the opposite sign, and a certain fraction of the previously absorbed energy is released as photons. There exists an additional mechanism in which localized transitions can take place between the electron and hole trapping states located in close proximity to each other, at separation distances of the order of tens of ångströms. In this case, the emission process takes place by thermal stimulation of the carrier into an excited state that is not in the conduction/valence band, and its subsequent recombination with its opposite-sign charge carrier is likely via a quantum-mechanical tunneling mechanism. In fact, it is quite probable that a mixture of localized and delocalized recombination simultaneously occurs in many TL materials. In the following, and for the sake of simplicity, the situation will be discussed in which electrons following excitation are in traps and therefore are mobile in the heating stage, whereas holes are in centers.

The TL Glow Curve

It deserves emphasis that TL arises from impurities in the host lattice (both desirable, purposely added in the growth process, and undesirable, e.g., present in the starting materials) at the ten to several hundred parts-per-million levels. This and other factors can give rise to impressively complicated glow curves as shown in Fig. 1 for LiF:Mg,Ti following electron and alpha particle irradiation, which is perhaps an extreme example. Notwithstanding this complexity, LiF:Mg,Ti is the most widely used of the dosimetric materials in which the integral of peaks 4–5 is commonly used as the measure of dose. Note the peak labeled "5a" is believed to arise from the localized transitions mentioned earlier and has been the subject of intensive investigation due to its ionization-density-dependent properties.

Mathematical Description of TL

The mathematics involved in the simulation of TL mechanisms consists of a complex series of multiple, non-linear, and coupled differential equations. The first theoretical derivation of $I(T)$ dealt with a highly idealized system consisting of a single trap and center. It was assumed that the thermally released electron immediately recombines with a hole in a center that yields a TL photon. The governing equation is

 http://dx.doi.org/10.1016/B978-0-12-409547-2.12096-7

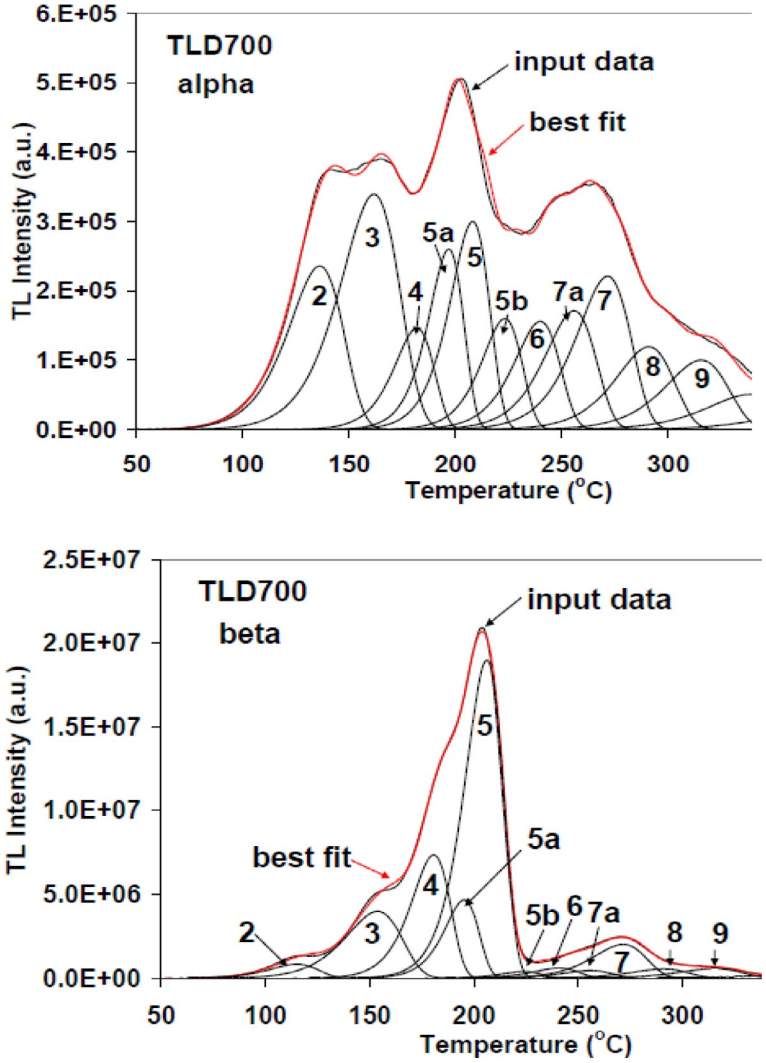

Fig. 1 (Top) The TL glow curve following irradiation by low-energy alpha particles and (bottom) by beta electrons. The glow curves have been deconvoluted into component glow peaks using peak shapes based on first-order kinetics.

$$I = -\frac{dn}{dt} = s \cdot n \cdot \exp\left(-E/kT\right) \tag{1}$$

where I is the intensity of emitted TL, n (cm^{-3}) the concentration of trapped electrons, s (s^{-1}) the frequency factor, E (eV) the activation energy, t (s) the time, T (K) the absolute temperature, and k ($\mathrm{eV \cdot K}^{-1}$) the Boltzmann constant. Assuming a linear heating function $T = T_0 + \beta t$ where β ($\mathrm{K \cdot s}^{-1}$) is the heating rate and T_0 (K) the initial temperature, the solution is a peak-shaped asymmetrical curve given by

$$I(T) = s \cdot n_0 \cdot \exp\left(-E/kT\right) \cdot \exp\left[-(s/\beta)\int_{T_0}^{T} \exp(-E/k\theta)d\theta\right] \tag{2}$$

where θ is a temperature dummy variable.

In 1948, Garlick and Gibson extended the theory to allow retrapping of electrons from the conduction band into the trap as discussed in the following within the broader framework of the one-trap–one-recombination center (OTOR) model.

Fig. 2 depicts a schematic energy-level diagram with one trapping state N and one kind of recombination center: M. N (cm^{-3}) and M (cm^{-3}) denote the concentrations of the traps and centers, respectively, and n (cm^{-3}) and m (cm^{-3}) their instantaneous concentration occupancies as a function of dose. Note that it is assumed in this framework that irradiation does not create new imperfections but rather fills existing traps and centers. n_c (cm^{-3}) and n_v (cm^{-3}) are the concentrations of free electrons and holes, respectively. A_m ($\mathrm{cm}^3\mathrm{s}^{-1}$) and A_n ($\mathrm{cm}^3\mathrm{s}^{-1}$) are the recombination and retrapping probability coefficients, respectively; B ($\mathrm{cm}^3\mathrm{s}^{-1}$) is the probability coefficient of trapping holes in the centers; and X ($\mathrm{cm}^{-3}\mathrm{s}^{-1}$) is the rate of production of electron–hole pairs by the radiation, which is proportional to the dose rate of excitation. The dashed lines show the transitions taking place during irradiation, and the solid lines represent transitions during heating. The set of coupled differential equations governing the process during excitation is

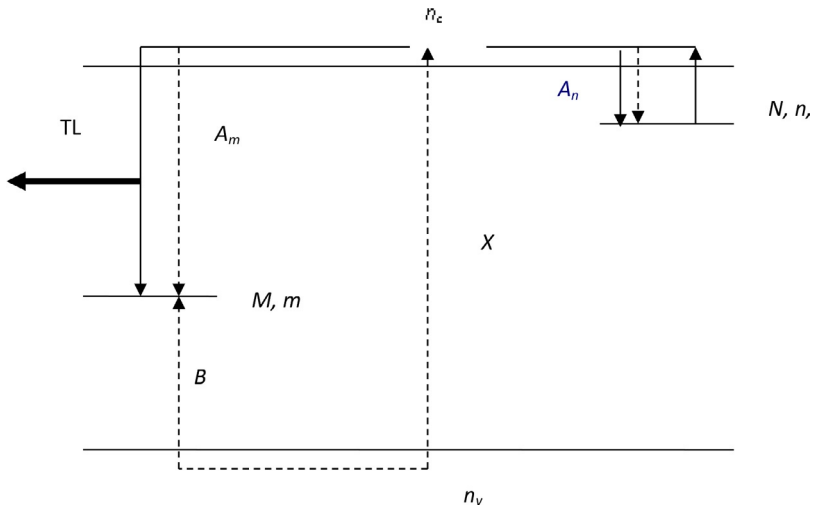

Fig. 2 Schematic energy-level diagram of a crystal with one trap, *N*, and one-recombination center *M*.

$$\frac{dn}{dt} = A_n(N-n)n_c - s\cdot n\cdot \exp(-E/kT) \tag{3}$$

$$\frac{dm}{dt} = B(M-m)n_v - A_m m n_c \tag{4}$$

$$\frac{dn_c}{dt} = X - A_n(N-n)n_c - A_m m n_c \tag{5}$$

$$\frac{dn_v}{dt} = \frac{dn}{dt} + \frac{dn_c}{dt} - \frac{dm}{dt} \tag{6}$$

This set of equations cannot be solved in a simple analytical manner. The optimum method is to solve numerically for a given set of parameters. For a complete description of the TL mechanism, the relaxation stage equations must also be solved (the relaxation stage refers to the time interval between excitation and heating when the remaining free electrons and holes retrap or recombine). The final stage of heating can then be simulated by solving the set of equations shown in the succeeding text, first developed in 1960 by Halperin and Braner and considered a reliable description of the OTOR model:

$$\frac{dn}{dt} = A_n(N-n)n_c - s\cdot n\cdot \exp(-E/kT) \tag{7}$$

$$I(T) = -\frac{dm}{dt} = A_m m n_c \tag{8}$$

$$\frac{dm}{dt} = \frac{dn}{dt} + \frac{dn_c}{dt} \tag{9}$$

Halperin and Braner also simplified Eqs. (7)–(9) in the following manner. If the concentration of free electrons is assumed rather small, that is, $n_c << n$ (which also implies that $m \sim n$), and the rate of change of this concentration is small, that is, $dn_c/dt \sim 0$, a single equation results:

$$I = -\frac{dm}{dt} = s\cdot n\cdot \exp(-E/kT)\cdot \frac{A_m m}{A_m m + A_n(N-n)} \tag{10}$$

It is evident that if recombination dominates, $A_m m >> A_n(N-n)$, Eq. (10) reduces to the Randall–Wilkins (Eq. (1)). If retrapping dominates, $A_m m << A_n(N-n)$, and if the trap is far from saturation, $N >> n$, one obtains the Garlick–Gibson second-order equation, that is,

$$I = -\frac{dn}{dt} = \frac{sA_m}{NA_n} n^2 \exp(-E/kT) \tag{11}$$

which yields a nearly symmetrical glow peak.

It is possible using the aforementioned analysis to easily evaluate the trapping parameters E and s, of single isolated glow peaks. The determination of the other parameters is more difficult but can be achieved by analyzing the shape of the peak, in particular, in the region of its initial increase in intensity (the "initial rise" region) or by the shift of the maximum temperature as a function of heating rate. Knowledge of these parameters can be useful in the estimation of the stability of the TL signal but should be regarded with caution due to "abnormal fading" and other complications as discussed by Chen.

Additional information on the dose filling constants and levels of concentration of the TCs can be obtained by optical absorption measurements following the irradiation stage. As for the properties of the recombination centers, the emission spectroscopy yields information on their properties.

From the aforementioned discussion, it should be evident that cases intermediate between first and second orders may occur. Furthermore, more often than not, several TL peaks will occur in a glow curve due to the many types of traps and centers in the material (Fig. 1). This results in significant complexity due to the competition between the different processes, an example of which is discussed in the following, when both localized and delocalized recombinations are treated in a multitrap, multicenter system describing LiF:Mg,Ti.

Dose–Response and Other TL Characteristics

The effects introduced by competition include non-linear dose dependence of the TL peak intensity. Whereas sublinear dose dependence is expected at relatively high doses due to the filling of existing traps and centers approaching saturation, superlinear dose dependence (Fig. 3) is also commonly observed and can be explained by competitive processes. In

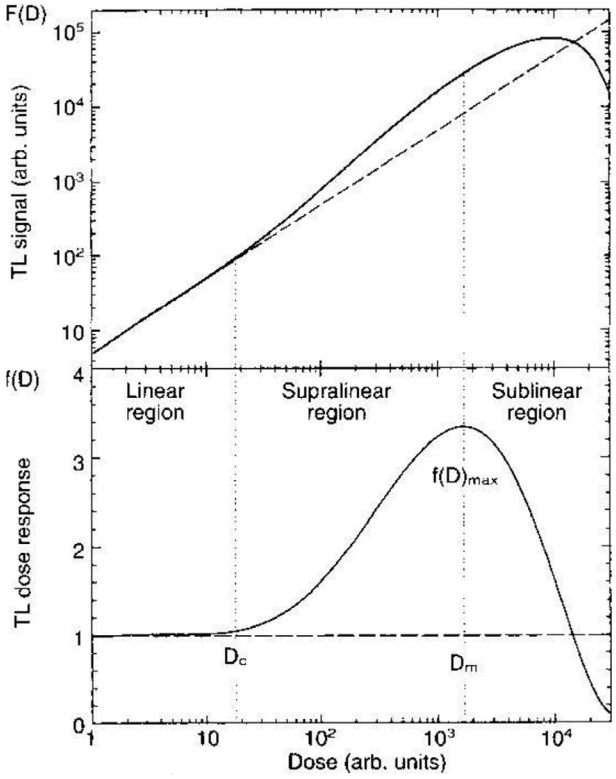

Fig. 3 The TL signal, $F(D)$, as a function of dose (top). The TL signal normalized to the signal at low dose, $f(D)$, in the linear response region (bottom). $f(D)$ is a measure of the TL efficiency.

addition, in many cases when superlinearity is observed, it can be dependent on the type and energy of the radiation, that is, on ionization density. In addition, the TL intensity is occasionally observed to be dependent on the applied dose rate, a behavior that can be simulated in systems with competing trapping states. Further unusual dose dependence of TL peaks has been reported, namely a non-monotonic dependence in which the TL peak intensity increases up to a certain dose, but then decreases at higher dose levels. Concentration quenching has been reported in several materials and can be important in the preparation of materials with maximum sensitivity. Although the occurrence of TL depends on the existence of impurities in the host sample, the sensitivity may first increase with the concentration of the dopant but then decrease. For example, in LiF:Mg,Ti, the optimum levels of concentration for dosimetric applications are a few hundred parts per million of Mg and ~10 ppm Ti. Many of these characteristics can be explained by the competition between different traps and/or centers and have been simulated by solving numerically the relevant sets of simultaneous differential equations.

Dosimetry via TL is an extremely useful tool due to the linear dose–response observed in some materials over many decades of response from ~μGy to ~Gy levels of dose. This extended range of linearity allows accurate measurement of dose in most environmental and personnel dosimetric applications. The deviation from linearity is a significant nuisance in clinical applications and other high-dose applications, but especially in the former, which usually requires exceptionally high precision and accuracy. LiF:Mg,Cu,P exhibits linearity up to levels of dose greater than 10 Gy before entry into saturation, but this material suffers somewhat from a loss in sensitivity when heated beyond 240 °C. Since the readout is incomplete at 240 °C, reuse requires recalibration due to the residual signal. Because LiF:Mg,Ti in its various forms is the most widely used of the dosimetric materials, our attention will be centered on the theoretical modeling of the dose–response ionization-density characteristics of this material.

Localized/Delocalized Recombination: The Effects of Ionization Density

Mathematical simulations like the OTOR model can only be applied to the TL mechanisms following uniform irradiation on a microscopic level, that is, by high-energy photon/electron radiation fields. Non-uniform irradiation leads to non-uniform population of the various centers following irradiation and relaxation, which can significantly change certain TL characteristics such as the glow curve (Fig. 1) and the behavior of the dose–response. It is now realized that linear/superlinear dose–response can best be described by a mixture of localized/delocalized recombination that arises from ionization-density-dependent population of TC/luminescent center (LC). Two approaches have been developed that deal with the challenges presented by non-uniform irradiation (both invoke nanodosimetric concepts based on spatially correlated TCs and LCs): (i) the unified interaction model (UNIM) including the extended track interaction model (ETIM) and (ii) conduction band/valence band kinetic models incorporating a mixture of localized and delocalized recombination.

The Unified Interaction Model

In these models, the fraction, n_{e-h}/n_e, of the density of e–h to e-only populated complexes (Fig. 4) following irradiation is given by

$$\frac{n_{e-h}}{n_e} = a\cdot\left(1 - e^{-\beta_{e-h}\cdot D}\right) + b \tag{12}$$

The combined densities must, of course, yield the total density of occupied peak 5 - TCs as given in the following:

$$n_{\text{tot}} = N_{\text{TC}}\left(1 - e^{-\beta_{\text{TC}}D}\right) = n_{e-h} + n_e \tag{13}$$

where β_{e-h} and β_{TC} are the dose filling constants of the e–h and the combined components of the TC/LC structure. These equations are employed to yield values of n_{e-h}/n_e that are approximately constant up to a demarcation dose of 1–10 Gy which is the threshold dose D_c where supralinearity begins to appear. The parameters a,b and β_{e-h} are postulated to depend on photon/electron energy.

The basic idea of the UNIM is that the linear response at low dose arises from geminate recombination in TC/LC correlated pair. For heavy charged particles (HCPs), the localized entity is the HCP track. The localized recombination process is unaffected by conduction band-mediated competitive processes.

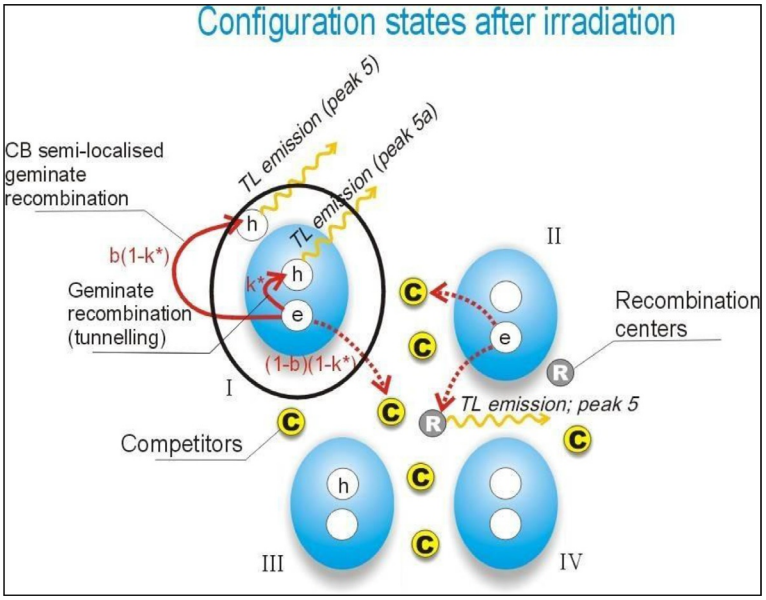

Fig. 4 Schematic representation of the spatially correlated TCs and LCs. As shown, there are four possible population configurations following irradiation. The *e–h* configuration gives rise to the linear dose–response.

The dependence on dose of the delocalized conduction band-mediated luminescence recombination gives rise to the supralinearity. As the dose increases, the average of the distance distribution between occupied/active neighboring TC/LC entities decreases, and the luminescence recombination efficiency increases due to the greater probability of charge carrier migration between neighboring TC/LC complexes without interception by the competitive centers (CCs). In addition, if the CCs during irradiation capture charge of the same sign as the TCs, their "competitive efficiency" is decreased as the dose level increases since an occupied CC no longer serves as an active CC for the charge carrier liberated by the TC.

The TL signal intensity, $F(D)$, is given by

$$F(D) = ksn_e(D) + (1-ks)n_e\sum_{i=1}^{3}\int_{r_0}^{r_{\max}} g(R)\cdot e^{-R/\lambda(D)}\cdot P_i(n_h,R,D)dR \quad (14)$$

It can be seen that $F(D)$ is composed of two terms, where ks is the contribution of the *e–h*-populated TC to the TL intensity that results in the linear part of the dose–response and $(1-ks)$ is the contribution that contributes to the supralinearity. The first term thus represents the contribution from localized (geminate) recombination and is linear/exponentially saturating due to the behavior of n_e with dose. The second term estimates the increased TL intensity at higher dose levels due to conduction band-mediated recombination in the presence of competitive processes. The parameters in Eq. (14) are defined as follows:

- n_e, n_{LC} (n_h), and n_{cc} represent the density of occupied TCs, LCs, and CCs, respectively, and their dose–response is described by a linear/exponentially increasing function of the form given by $N_i\cdot[1-\exp^{(-\beta iD)}]$.
- r_0 is the radius of the TC/LC complex.
- $g(r_h.R_i)$ is a two-dimensional solid-angle factor between two neighboring TC/LC pairs.
- R_i is the distance between neighboring TC/LC pairs.
- λ, the mean free path of the electrons between the TC/LC pairs, is an increasing function of dose (due to the filling (deactivation) of the competitors with increasing dose) and is given by

$$\lambda(D) = \lambda_0\, e^{\beta_{cc}D} \quad (15)$$

- λ_0 is the mean free path for charge carrier diffusion in the intertrack un-irradiated region.
- β_{cc} is the dose filling constant of the CC in the TL recombination stage.

The nearest-neighbor probability distribution functions, $P_i(n_{LC},R_i)dR_i$, are a crucial element in the calculation of $F(D)$ since it is over these distances that the electron must migrate in the conduction band before recombination with a hole trapped in a LC. $F(D)$ is calculated using the sum of the first, second, and third nearest-neighbor interactions. The critical level of dose for composite peak 5 above which supralinearity occurs is ~1 Gy, above which $f(D)>1$ reaching values of ~3–5 at dose levels of ~200 Gy as shown in Fig. 5. The solid lines are theoretical fits using either the UNIM or the localized/delocalized band modeling.

Band Theory Kinetics Including Localized Recombination

The second approach is also capable of describing all of the dose–response characteristics of composite peak 5 in LiF:Mg, Ti. Details of the band model in the recombination stage are shown in Fig. 6.

The equations governing charge carrier transport between the various entities are similar to those detailed in Eqs. (7)–(10) and have been solved using MATLAB® code 23 s from The MathWorks Inc. In order to describe all the

dose–response characteristics of peaks 5a and 5 comprising composite peak 5, it was necessary to introduce the presence of band–tail states into the kinetic model. These states are believed to arise by fluctuations in bonding angle throughout the crystal, which generate localized shallow states below the high mobility conduction band edge. The presence of band–tail states has been invoked in other luminescent phenomena in feldspar and geminate recombination in hydrogenated amorphous silicon. In order to allow tunneling between the continuum of these states, the wavefunction of the trapped electrons must extend beyond the potential well boundaries. The trapped electron in the ground state is thermally elevated into the continuum of the band–tail states (the details of the energy distribution of the continuum are not essential to the modeling), and recombination proceeds directly from the band–tail states to the recombination center. In addition, as shown in Fig. 6, electrons can also be thermally elevated from the ground state to the conduction band, and recombination follows migration in the conduction band.

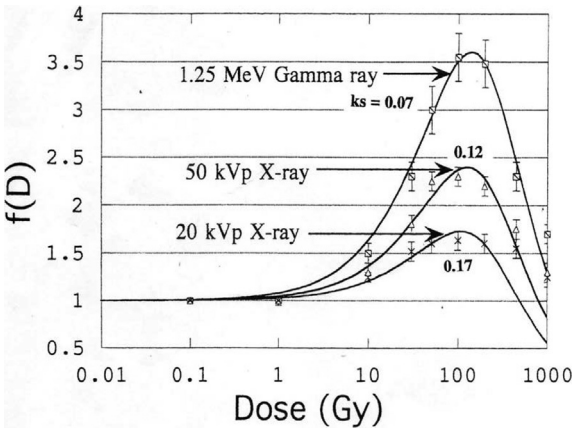

Fig. 5 Experimentally measured values of $f(D)$ at three photon energies. Note the decrease of $f(D)_{max}$ with decreasing photon energy. The full lines are theoretical fits using the UNIM.

Advances in Analysis: Impact on Applications

Applications of TL

The main applications of TL occasionally combined with optically stimulated luminescence (OSL) are dosimetry and the dating of archeological and geologic samples. In archeology, the time elapsed since the last firing (usually during production) of ancient pottery is measured by evaluating the accumulated dose to the shard following firing. In geology, the date is assumed to apply to the last exposure to light. Both applications require the determination of the absorbed dose from radioactive sources over the intervening time interval; ergo, dating is considered a dosimetric application.

In both dosimetry and dating, various interrelated considerations are involved in the choice of the optimum material. These include the following:

1. High sensitivity to noise/background: In order to obtain useful minimum measurable levels of dose, this quality factor may be dependent on the type of radiation.
2. Reproducibility/sample to sample consistency:

   In some materials, a cycle of irradiation followed by heating may change the sensitivity of the material to a subsequent irradiation. This is a common problem with different kinds of quartz, a material that is widely used in dating. In commercially supplied dosimeters, it is often necessary to preselect from a population of dosimeters in order to achieve the desired precision.

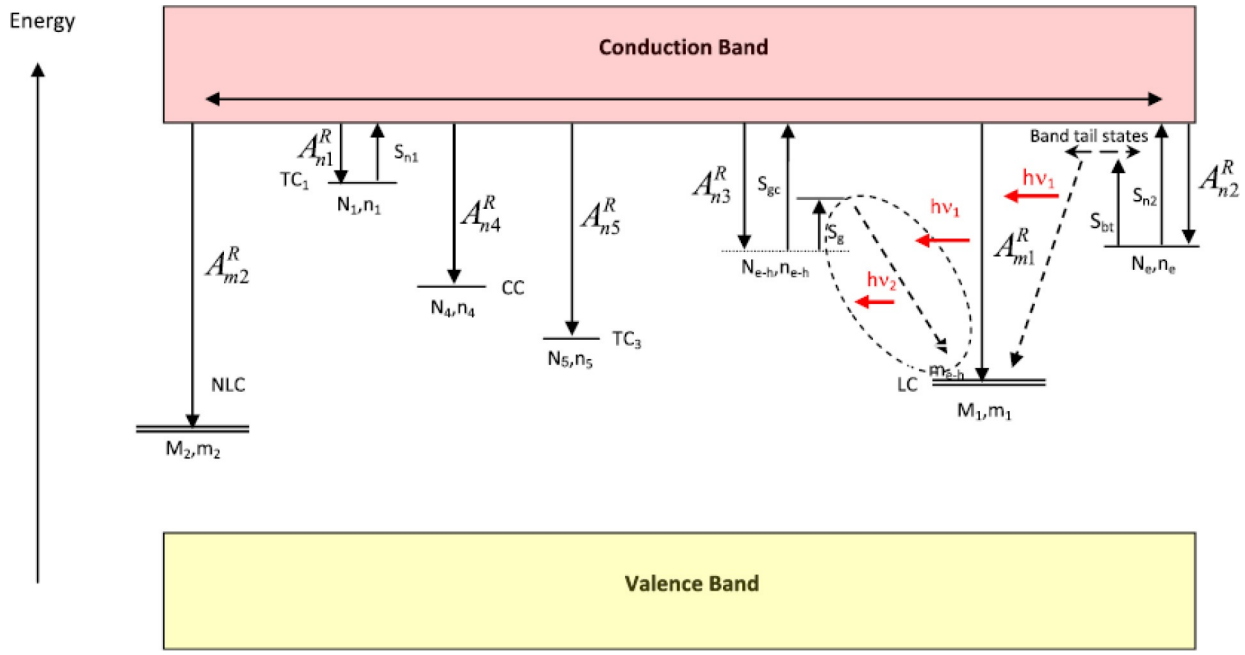

Fig. 6 Recombination stage band model for TC/LC spatially correlated pairs. For a full explanation, the reader is referred to the chapter by Eliyahu et al.

3. Dose–response linearity and dose-rate independence: A linear response is highly preferable since it greatly reduces problems of calibration. Dose-rate independence is also highly desirable — most studies seem to indicate that this feature is not a problem for most applications.
4. Stability: In both dosimetry and dating applications, some time may elapse between exposure to radiation and readout. In addition, the duration of irradiation may influence the calibration if the signal is unstable. It is usually observed that high-temperature glow peaks are more stable with time — in LiF:Mg,Ti, the so-called dosimetric peak, appearing at approximately 200 °C, does not "fade" by more than 5% annually.

The choice of an "ideal" TL dosimeter is a compromise between all these characteristics. Even in conventional applications such as personal and environmental dosimetry, reasonably precise and accurate dosimetry requires frequent batch and individual recalibration. Although one might assume that, for example, LiF:Mg,Ti with known optimal Mg,Ti concentrations would have universal characteristics, this is not the case. The TL properties of LiF:Mg,Ti from different sources can be substantially different, and even from the same source, the characteristics may vary over the years. The main materials in use are LiF:Mg,Ti (TLD-100); CaF_2:Dy (TLD-200); CaF_2:Tm (TLD-300); CaF_2:Mn (TLD-400); Al_2O_3:C (TLD-500); LiF:Mg,Ti with enriched ^{6}Li, sensitive to thermal neutrons (TLD-600); LiF:Mg,Ti with enriched ^{7}Li, insensitive to thermal neutrons (TLD-700); Li_2BO_7 (TLD-800); and $CaSO_4$:Dy (TLD-900). Notwithstanding the problems mentioned earlier, millions of these dosimeters are in constant use worldwide.

The situation with archeological and geologic dating and in retrospective dosimetry following nuclear accidents is more difficult. One has to use natural materials and cope with possibly wide variations in the properties of materials such as quartz grains and feldspars. For retrospective dosimetry, the use of ceramic materials in electronic components such as cellular phones and flash drives as well as common household salts has been suggested.

Methods of Analysis

The simplest method to quantify the TL signal is to measure the integral of the emitted light over a temperature interval, ΔT. In all the other methods, the glow curve, that is, $I(T)$ or alternately the simpler to measure, $I(t)$, is recorded, and the signal to be correlated with dose is based on some form of computerized glow curve analysis (CGCA). The following are several options to analyze the TL signal:

(i) Measure the peak height of the dosimetric peak. This method has some possible disadvantages. At low dose, the peak height can suffer from statistical fluctuations much greater than for an integrated TL signal, and in the case of complex glow curves, the peak height may be influenced by neighboring/overlapping peaks whose dosimetric characteristics are different.
(ii) A second method is based on integration of the TL signal between two predetermined temperatures that define the so-called region of interest (ROI). More than one ROI may be applied simultaneously. This method alleviates the statistical fluctuations suffered by peak height methods but is still based on the overlap of several peaks and on the subjective choice of the temperature of the valley that may move around due to instrumental fluctuations.
(iii) A third method, the so-called simplified CGCA, analyzes the glow curve shape or profile and compares with previously recorded glow curves.
(iv) Finally, the fourth method is to carry out "full-blown" computerized glow curve deconvolution (CGCD) into component glow peaks. The choice of the method of analysis is based on the requirements of the application — some require speed/high throughput, and others may require extremely high precision.

CGCA has been successfully applied to many issues: (i) characterization of new materials, (ii) glow curve characteristics affecting sensitivity changes and fading, (iii) dose–response of individual glow peaks, (iv) effects of heating rate, (v) deconvolution of HCP-induced glow curves, (vi) mixed-field dosimetry, and (vii) microdosimetric and nanodosimetric interpretation of glow curve characteristics and others.

See also: Atomic Absorption, Theory; Atomic Emission and Fluorescence Theory; Atomic Fluorescence, Methods and Instrumentation; Chiroptical Spectroscopy, Emission Theory; Chiroptical Spectroscopy, General Theory; Circularly Polarized Luminescence and Fluorescence Detected Circular Dichroism; Colorimetry, Theory; Electromagnetic Radiation; Electron Diffraction Theory and Methods; EPR Spectroscopy, Theory; Fluorescence Microscopy, Applications; Fluorescence Polarization and Anisotropy; Fluorescence Spectroscopy, Biochemical Applications; Fluorescence Spectroscopy, Organic Chemistry Applications; Fluorescence Theory; Fluorescence up-conversion Methods and Applications; Fluorescent Molecular Probes; Fourier Transformation and Sampling Theory; Ion Collision, Theory; IR Spectroscopy, Theory; Laser Spectroscopy Theory; Luminescence Spectroscopy, Inorganic Condensed Matter Applications; Luminescence, Theory; Magnetic Circular Dichroism, Theory; Mass Spectrometry, Ionization Theory; MRI Theory; Mössbauer Spectroscopy, Theory; Multivariate Statistical Methods; Neutron Diffraction, Theory; NMR in Anisotropic Systems, Theory; Nonlinear Raman Spectroscopy, Theory; Nuclear Quadrupole Resonance, Theory; Optical Spectroscopy, Linear Polarization Theory; Parameters in NMR Spectroscopy, Theory of; PET, Theory; Photoacoustic Spectroscopy, Theory; Photoelectron Spectroscopy, Zero Kinetic Energy, Theory; Plasmon-Controlled Fluorescence Methods and Applications; Radiofrequency Field Gradients in NMR, Theory; Raman Optical Activity, Theory; Rayleigh Scattering and Raman Effect, Theory; Rotational Spectroscopy, Theory; Scanning Probe Microscopy, Theory; Scattering Theory; Statistical Theory of Mass Spectra; Statistical Tools for Molecular Covariance Spectroscopy; Statistics for Spectroscopy; Super-Resolution Fluorescence Microscopy, Localization Microscopy; Surface Plasmon Resonance, Theory; Symmetry and Spectroscopy; Symmetry in Crystallography; Symmetry in Spectroscopy, Effects of; Tensor Representations; Terahertz spectroscopy theory; UV–Visible Fluorescence Spectrometers; Vibrational CD, Theory and Application to Determination of Absolute Configuration; Vibrational CD, Theory; X-Ray Crystallography of Macromolecules, Theory and Methods; X-ray Crystallography of Small Molecules: Theory and Workflow; X-Ray

Fluorescence Spectrometers; X-Ray Fluorescence Spectroscopy, Applications; X-Ray Spectroscopy, Theory.

Further Reading

Wick FG (1927) *JOSA* 14: 33–44.
Randall JT and Wilkins MHF (1945) *Proc. Roy. Soc. A* 184: 347–407.
Horowitz YS (1984) *Thermoluminescence and Thermoluminescent Dosimetry*Vols. I, II, III. Boca Raton, FL: CRC Press.
McKeever SWS, Moscovitch M, and Townsend PD (1995) *Thermoluminescence Dosimetry Materials: Properties and Uses*. UK: Nuclear Technology Publishing.
Braunlich P (ed.) (1979) In: *Topics in Applied Physics, Thermally Stimulated Relaxation in Solid*, vol. 37. Berlin/New York: Springer Verlag.
Horowitz YS, Oster L, Biderman S, and Einav Y (2003) *J. Phys. D. Appl. Phys.* 36: 446–459.
Garlick GFJ and Gibson AF (1948) *Proc. Phys. Soc.* 60: 574–590.
Halperin A and Braner AA (1960) *Phys. Rev.* 117: 408–415.
Chen R and Pagonis V (2011) *Thermally and Optically Stimulated Luminescence: A Simulation Approach*. Chichester: Wiley.
Aitken MJ (1985) *TL Dating*. London/Orlando: Academic Press.
Horowitz YS (2001) *Nucl. Instrum. Meth*. B184: 68–84.
Horowitz YS, Avila O, and Rodrígues-Villafuerte M (2001) *Nucl. Instrum. Meth.* B184: 85–112.
Eliyahu I, Horowitz YS, Oster L, and Mardor I (2014) *J. Lumin.* 145: 600–607.
Jain M and Ankjærgaard C (2011) *Radiat. Meas.* 46: 292–309.
The International Conferences on Solid State Dosimetry, www.issdo.org.
Horowitz YS and Yossian D (1995) *Radiat. Prot. Dosim.* 60: 1–114.
Horowitz YS and Moscovitch M (2013) *Radiat. Prot. Dosim.* 153: 1–22.
Chen R and Hag-Yahya A (1997) *Radiat Meas*. 27: 205–210.